s- and *p*-wave pairings in the dilute electron gas: Superconductivity mediated by the Coulomb hole in the vicinity of the Wigner-crystal phase

Yasutami Takada
Institute for Solid State Physics, University of Tokyo, 7-22-1 Roppongi, Minato-ku, Tokyo 106 Japan
(Received 18 June 1992; revised manuscript received 25 September 1992)

The superconducting transition temperature T_c of both *s*- and *p*-wave pairings is calculated in the electron gas without phonons by the solution of the full Eliashberg equation in both frequency and momentum variables. The exchange and correlation effects are included in the form of the model proposed by Kukkonen and Overhauser with suitable local-field corrections. The ground state of the electron gas exhibits *p*-wave superconductivity for the electronic-density parameter r_s around 4 or larger, but it is superseded by *s*-wave superconductivity for r_s larger than about 8.5. The ratio of T_c to the Fermi energy increases monotonically with r_s, but it is saturated to have the value of about 0.04 for $r_s > 40$. The physical origin of this superconductivity in the dilute electron gas is explained in terms of the pairing mediated by the Coulomb hole near the Wigner-crystal phase.

I. INTRODUCTION

Superconductivity in the electron gas without phonons has been a matter of controversy ever since Kohn and Luttinger[1] discussed a possibility of *p*- or *d*-wave Cooper pairs with the use of the Friedel oscillation. A possibility of *s*-wave superconductivity was pointed out with the help of the plasmons by the present author[2] and this plasmon mechanism is the main topic of subsequent works.[3–13] Recently, the plasmon mechanism is confirmed in the many-valley electron gas by the solution of the full Eliashberg equation[14] in which both the one-particle Green's function G and irreducible two-electron interaction $\tilde{I}$ are evaluated systematically in the g_v^{-1} expansion where g_v is the valley degeneracy.[13] This expansion amounts to the calculation of G and $\tilde{I}$ in the random-phase approximation (RPA) in first order of g_v^{-1} and a strong cancellation works among the terms in its second order. In the analysis, *s*-wave superconductivity appears for $g_v \geq 2$ even in the region of the electronic-density parameter r_s less than unity where the RPA is guaranteed to be a very good approximation.

The conclusion in Ref. 13, however, cannot be applied to the usual electron gas in which $g_v = 1$. Thus, we still do not know whether the electron gas exhibits superconductivity without phonons or not. A strong argument exists against superconductivity by referring to the experimental fact that the alkali metals do not show superconductivity. It is true that those metals are considered to be ideal realization of the electron gas in many respects, but they are not the same as the electron gas. For example, the compressibility κ is enhanced much over the free-electron value κ_F in the electron gas and becomes negative for $r_s > 5.3$, whereas values of κ in the alkali metals are not large and even smaller than κ_F for the heavy alkali metals such as K, Rb, and Cs. (Note that an experimental support has been given recently for the negative κ in the electron gas in two dimension.[15]) Since κ measures the strength of the response to charge fluctuations, suppression of κ in the alkali metals has probably a fatal effect on superconductivity in such a charge-fluctuation mechanism as the plasmon one. Thus, in discussing superconductivity in the electron gas, we should not have such a prejudice in the first place as found in Refs. 3–5, 10, and 12 in which the obtained superconducting solution was asserted to be erroneous or artifact without any clear reasons other than the absence of superconductivity in the alkali metals.

To obtain a deeper insight into the physical origin of the plasmon mechanism of superconductivity, we have made a detailed examination as to the condition of its occurrence in the many-valley electron gas in the range $0 < r_s < 1$. As a result, we find that the most important parameter is the ratio of the plasma energy ω_p to the Fermi energy E_F: Superconductivity appears only if ω_p/E_F is larger than about 3. A stronger superconducting instability is obtained for even larger values of ω_p/E_F. We note that this is a completely different situation from the conventional phonon mechanism of superconductivity in which the characteristic energy ω_0 for the modes to be exchanged by the Cooper pair is much smaller than E_F.

It is usually argued that Migdal's theorem[16] can be applied only to the case of $\omega_0 \ll E_F$. It is true that for $\omega_0 \approx E_F$, vertex corrections play an important role. But they do not seem to give a large contribution at the other extreme $\omega_0 \gg E_F$, because complicated processes as described by the vertex corrections cannot be important in a high-energy region. Thus we can expect that a proper account of the plasmon contribution to superconductivity is already made in the approximation without vertex corrections, namely, the RPA, if ω_p/E_F is large. Since the condition of $\omega_p/E_F > 3$ corresponds to that of $r_s > 10$ for the electron gas with $g_v = 1$, *s*-wave superconductivity may appear in the dilute electron gas, i.e., $r_s > 10$ even if we make a more realistic calculation in which vertex corrections are included in an appropriate way.

Motivated by the above idea, we have looked into the works in which the vertex corrections are claimed to des-

troy superconductivity once obtained in the RPA. Among those works, the one by Büche and Rietschel[12] (BR) is most serious and important. [The work by Grabowski and Sham[4] (GS) had an error and corrected their results later.[8] Canright and Vignale[10] followed the suggestion of GS and they did not solve the full Eliashberg equation faithfully.] BR solved the full Eliashberg equation in both frequency and momentum variables. The vertex corrections were taken into account by the model proposed originally by Kukkonen and Overhauser (KO).[17] BR found no superconducting solution in the electron gas in the model.

The conclusion of BR cannot be a conclusive one mainly for the following two reasons: The first one is concerned with the range of r_s. BR considered the case of $1 \le r_s \le 5$, whereas we expect the plasmon mechanism of s-wave superconductivity for $r_s > 10$. Thus we need to extend the work of BR into the region of larger r_s. The second reason is related to the pairing nature. BR considered only s-wave pairing, but once we take account of the vertex corrections including the contribution from paramagnons, p-wave pairing should be investigated as well. In fact, even in the RPA, p-wave pairing was found to dominate for $2.3 < r_s < 4.7$ in the electron gas with $g_v = 1$.[13]

In view of those situations, we review the paper of BR critically and extend their work to the larger-r_s case. In addition, p- as well as s-wave pairing is treated in this paper. We make a detailed consideration on the physical origin of this superconductivity in the low-density limit, namely, from the side of the Wigner-crystal phase and try to validate the plasmon mechanism of superconductivity in terms of the pairing mediated by the Coulomb hole in the very strongly-correlated electron gas.

This paper is organized as follows: In Sec. II, we formulate the problem and give a very brief description of our numerical procedure. In Sec. III, we discuss our results for the normal-state properties, while in Sec. IV, we give those of superconductivity including T_c. The physical origin of the plasmon mechanism in the dilute electron gas is discussed in Sec. V. In Sec. VI, we summarize our results and discuss problems relating to the concepts proposed in this paper. In the following, we employ units in which $\hbar = k_B = 1$.

II. FORMULATION

A. Hamiltonian

The electron gas is a system consisting of N electrons embedded in a uniform positive-charge background. The electrons interact with one another through the Coulomb interaction with the dielectric constant ε_0. With the effective mass m^*, we can write the Hamiltonian in second quantization as

$$H = \sum_{\mathbf{k}\sigma} \varepsilon_{\mathbf{k}} C^{\dagger}_{\mathbf{k}\sigma} C_{\mathbf{k}\sigma} + \frac{1}{2} \sum_{\mathbf{q}\neq 0} \sum_{\mathbf{k}\sigma} \sum_{\mathbf{k}'\sigma'} V(q) C^{\dagger}_{\mathbf{k}+\mathbf{q}\sigma} C^{\dagger}_{\mathbf{k}'-\mathbf{q}\sigma'} C_{\mathbf{k}'\sigma'} C_{\mathbf{k}\sigma}, \tag{2.1}$$

where $\varepsilon_{\mathbf{k}} = \mathbf{k}^2/2m^* - \mu$ with the chemical potential μ and $V(q) = 4\pi e^2/\varepsilon_0 q^2$. The volume of the system is taken to be unity. The operator $C_{\mathbf{k}\sigma}$ represents the annihilation of an electron with momentum $\mathbf{k}$ and spin σ. The system can be specified by $r_s \equiv 1/\alpha a_B^* k_F$ with $\alpha = (4/9\pi)^{1/3} = 0.521$, the effective Bohr radius $a_B^* \equiv \varepsilon_0/m^* e^2$, and the Fermi momentum $k_F \equiv (3\pi^2 N)^{1/3}$. Appropriate scales for momenta and energies are, respectively, k_F and the Fermi energy $E_F \equiv k_F^2/2m^*$. Temperatures will be given in units of effective kelvin $\mathrm{K}^* \equiv (m^*/m_e \varepsilon_0^2)\mathrm{K}$ where m_e is the mass of a free electron.

B. Eliashberg equation

The formally exact gap equation at $T = T_c$ is written as[13,14]

$$\phi(\mathbf{k}, i\omega_n) = T \sum_{\omega_{n'}} \sum_{\mathbf{k}'} \frac{\tilde{I}_{\sigma\sigma'}(\mathbf{k}, i\omega_n; \mathbf{k}', i\omega_{n'}) \phi(\mathbf{k}', i\omega_{n'})}{[i\omega_{n'} Z(k', i\omega_{n'})]^2 - [\varepsilon_{k'} + \chi(k', i\omega_{n'})]^2}, \tag{2.2}$$

where $\omega_n \equiv \pi T(2n+1)$ is the Matsubara frequency with an integer n, the gap function $\phi(\mathbf{k}, i\omega_n)$, the level-shift $\chi(k, i\omega_n)$, and the renormalization function $Z(k, i\omega_n)$ are real and even in ω_n, and $\tilde{I}_{\sigma\sigma'}(\mathbf{k}, i\omega_n; \mathbf{k}', i\omega_{n'})$ is the irreducible electron-electron interaction for scattering from the state specified by $(i\omega_n \mathbf{k}\sigma, -i\omega_n - \mathbf{k}\sigma')$ into that by $(i\omega_{n'} \mathbf{k}'\sigma, -i\omega_{n'} - \mathbf{k}'\sigma')$. With the normal-state self-energy $\Sigma(k, i\omega_n)$, $\chi(k, i\omega_n)$ and $Z(k, i\omega_n)$ are given by

$$\chi(k, i\omega_n) = \tfrac{1}{2}[\Sigma(k, i\omega_n) + \Sigma(k, -i\omega_n)], \tag{2.3}$$

and

$$i\omega_n [1 - Z(k, i\omega_n)] = \tfrac{1}{2}[\Sigma(k, i\omega_n) - \Sigma(k, -i\omega_n)], \tag{2.4}$$

respectively. Owing to the spherical symmetry in $\mathbf{k}$ space, these functions depend on $\mathbf{k}$ only through $k \equiv |\mathbf{k}|$.

C. Kukkonen-Overhauser model

In order to obtain proper forms for $\Sigma(k, i\omega_n)$ and $\tilde{I}_{\sigma\sigma'}(\mathbf{k}, i\omega_n; \mathbf{k}', i\omega_{n'})$ with the effects of exchange and correlation, we adopt the model proposed by KO for the effective electron-electron interaction $V_{\sigma,\sigma'}(q, \omega)$, which describes the scattering of two electrons with spins σ and σ' for momentum and energy transfers $(\mathbf{q}, \omega)$ in the electron gas.[17] In the scheme, $V_{\sigma,\sigma'}(q, \omega)$ is composed of the bare interaction $V(q)$ and the interactions mediated by charge and spin fluctuations as

$$V_{\sigma,\sigma'}(q, \omega) = V(q) + V_+(q)^2 Q_+(q, \omega) + V_-(q)^2 Q_-(q, \omega) \boldsymbol{\sigma} \cdot \boldsymbol{\sigma}' . \tag{2.5}$$

Here $Q_+(q, \omega)$ and $Q_-(q, \omega)$ are, respectively, the charge and spin response functions, given by

$$Q_{\pm}(q, \omega) = -\frac{\Pi(q, \omega)}{1 + V_{\pm}(q) \Pi(q, \omega)}, \tag{2.6}$$

with the polarization function $\Pi(q, \omega)$ evaluated in the

RPA. The couplings of electrons with those fluctuations are given by $V_{\pm}(q)$, which are defined with the use of the so-called local-field correction $G_{\pm}(q)$ as

$$V_{+}(q)\equiv[1-G_{+}(q)]V(q), \tag{2.7}$$

and

$$V_{-}(q)\equiv[-G_{-}(q)]V(q). \tag{2.8}$$

We can choose the forms of $G_{\pm}(q)$ at our disposal, provided that they satisfy the following conditions at $q=0$ and ∞:

$$\lim_{q\to 0}[1-G_{+}(q)V(q)\Pi(q,0)]=\frac{\kappa_F}{\kappa}, \tag{2.9}$$

$$\lim_{q\to 0}[1-G_{-}(q)V(q)\Pi(q,0)]=\frac{\chi_F}{\chi}, \tag{2.10}$$

$$\lim_{q\to\infty} G_{+}(q)=\tfrac{2}{3}-\tfrac{1}{3}g^{\uparrow\downarrow}(0), \tag{2.11}$$

and

$$\lim_{q\to\infty} G_{-}(q)=\tfrac{2}{3}g^{\uparrow\downarrow}(0)-\tfrac{1}{3}, \tag{2.12}$$

where κ and χ are, respectively, the compressibility and the spin susceptibility of the electron gas, κ_F and χ_F are their values in the noninteracting case, and $g^{\uparrow\downarrow}(0)$ is the spin-antiparallel pair distribution function at zero separation. The first two equations in the above are, respectively, derived from the compressibility sum rule and the corresponding one for χ. The third one is due to Niklasson,[18] while the last one is given by Zhu and Overhauser.[19]

In this paper, we assume the form for $G_{\pm}(q)$ as

$$G_{\pm}(q)=\frac{A_x q^2}{k_F^2+B_x q^2}\pm\frac{A_c q^2}{k_F^2+B_c q^2}. \tag{2.13}$$

The four coefficients, A_x, B_x, A_c, and B_c, can be determined by the conditions of (2.9)–(2.12). The values of κ_F/κ and χ_F/χ are given as the function of r_s in Ref. 20 and those of $g^{\uparrow\downarrow}(0)$ are found in Ref. 21. Note, however, that rather different values of χ_F/χ are obtained in a recent paper.[22] Since we believe that they are better, the values of Ref. 22 are used for χ_F/χ. Approximate formulas for those quantities are written as

$$\frac{\kappa_F}{\kappa}=1-\frac{\lambda^2}{4}\left[1+0.07671\lambda^2\frac{(1+a_1\lambda)^2+\frac{4}{3}a_2\lambda^2(1+\frac{7}{8}a_1\lambda)+\frac{3}{2}a_3\lambda^3(1+\frac{8}{9}a_1\lambda)}{(1+a_1\lambda+a_2\lambda^2+a_3\lambda^3)^2}\right], \tag{2.14}$$

$$\frac{\chi_F}{\chi}=1-\frac{\lambda^2}{4}\left[1+\frac{\lambda^2}{8}\left[\ln\frac{\lambda^2}{\lambda^2+0.990}-\frac{1.122+1.222\lambda^2}{1+0.533\lambda^2+0.184\lambda^4}\right]\right], \tag{2.15}$$

and

$$g^{\uparrow\downarrow}(0)=\left[\sum_{n=0}^{\infty}\frac{\lambda^{2n}}{n!(n+1)!}\right]^{-2}, \tag{2.16}$$

with $\lambda\equiv(4\alpha r_s/\pi)^{1/2}$, $a_1=12.05$, $a_2=4.254$, and $a_3=1.363$.

An attempt was made by Vignale and Singwi (VS) to justify the form (2.5) from a microscopic point of view.[23] VS obtained the almost same form as (2.5), but they claimed some difference in the term concerning transverse spin fluctuations from that in KO. However, their claim is not totally correct and we can employ (2.5) as it is. An inconsistent treatment of longitudinal and transverse spin fluctuations in VS resulted in such a claim. Incidentally, Eq. (20) in Ref. 12 shows clearly that BR did not include the interaction mediated by transverse spin fluctuations. An exact reason is not known for this omission, but this produces a difference in the prefactor for the contribution of spin fluctuations to both $\Sigma(k,i\omega_n)$ and $\tilde{I}_{\sigma\sigma'}(\mathbf{k},i\omega_n;\mathbf{k}',i\omega_{n'})$. Numerically, however, this difference is not expected to be serious at all. Contrary to the Hubbard model, the correlation effect enhances the charge response, while it reduces the spin response so much that the effect of spin fluctuations is small in the electron gas.

D. Self-energy

In the model of KO, an electron is moving in the medium described by (2.5). Since the electron can make virtual emission and absorption of charge and/or spin fluctuations repeatedly, we have to determine the self-energy $\Sigma(k,i\omega_n)$ in a self-consistent manner as[24]

$$\Sigma(k,i\omega_n)=-T\sum_{\omega_{n'}}\sum_{\mathbf{k}'}[V(|\mathbf{k}-\mathbf{k}'|)+V_{+}(|\mathbf{k}-\mathbf{k}'|)^2Q_{+}(|\mathbf{k}-\mathbf{k}'|,i\omega_n-i\omega_{n'})$$
$$+3V_{-}(|\mathbf{k}-\mathbf{k}'|)^2Q_{-}(|\mathbf{k}-\mathbf{k}'|,i\omega_n-i\omega_{n'})]G(k',i\omega_{n'}), \tag{2.17}$$

where the full Green's function $G(k,i\omega_n)$ is defined with the use of the bare one $G^{(0)}(k,i\omega_n)=(i\omega_n-\varepsilon_{\mathbf{k}})^{-1}$ and $\Sigma(k,i\omega_n)$ as

$$G(k,i\omega_n)\equiv[G^{(0)}(k,i\omega_n)^{-1}-\Sigma(k,i\omega_n)]^{-1}$$
$$=[i\omega_n Z(k,i\omega_n)-\varepsilon_{\mathbf{k}}-\chi(k,i\omega_n)]^{-1}. \quad (2.18)$$

The factor 3 in front of the spin-fluctuation term reflects the existence of one longitudinal and two transverse modes. We will solve (2.17) by an iteration method with an initial input of $\Sigma(k,i\omega_n)=0$.

Physically, the use of the full Green's function in the right-hand side of (2.17) is reasonable and in fact this self-consistency is important to obtain the proper damping effect in the plasma-energy region. However, as noted first by DuBois,[25] a strong cancellation works among vertex corrections and self-energy terms for the physical quantities near the Fermi surface.[26] Thus the self-energy evaluated with $G^{(0)}(k',i\omega_{n'})$ in (2.17) in place of $G(k',i\omega_{n'})$, i.e., $\Sigma(k,i\omega_n)$ after the first step of the iteration loop might be better than that obtained after the full iteration loop. For this reason, we will calculate the superconducting as well as normal-state properties with both of those Σ's. In Secs. III and IV, the symbols with KO-G and KO-$G^{(0)}$ will designate the results obtained with the full Green's function G and the bare one $G^{(0)}$ in (2.17), respectively.

E. Gap equation

In the present model for the effective electron-electron interaction, the gap equation (2.2) can be written as

$$\phi(\mathbf{k},i\omega_n)=T\sum_{\omega_{n'}}\sum_{\mathbf{k}'}\frac{\phi(\mathbf{k}',i\omega_{n'})}{[i\omega_{n'}Z(k',i\omega_{n'})]^2-[\varepsilon_{k'}+\chi(k',i\omega_{n'})]^2}[V(|\mathbf{k}-\mathbf{k}'|)+V_+(|\mathbf{k}-\mathbf{k}'|)^2Q_+(|\mathbf{k}-\mathbf{k}'|,i\omega_n-i\omega_{n'})$$
$$-3V_-(|\mathbf{k}-\mathbf{k}'|)^2Q_-(|\mathbf{k}-\mathbf{k}'|,i\omega_n-i\omega_{n'})], \quad (2.19)$$

for spin-singlet pairing and a similar equation is given for the spin-triplet case in which the factor -3 in front of the spin-fluctuation term in (2.19) is replaced by $+1$.

A further reduction can be made for (2.19) by an angular momentum decomposition of $\phi(\mathbf{k},i\omega_n)$. Since the interaction depends on $\mathbf{k}$ and $\mathbf{k}'$ only through $|\mathbf{k}-\mathbf{k}'|$, the decomposition can be done with the spherical harmonics $Y_{lm}(\theta,\phi)$ with $m=0$. Then we obtain an equation to determine the l-wave gap function $\phi_l(k,i\omega_n)$ as

$$\phi_l(k,i\omega_n)=T\sum_{\omega_{n'}}\sum_{\mathbf{k}'}\frac{I_l(k,i\omega_n;k',i\omega_{n'})\phi_l(k',i\omega_{n'})}{[i\omega_{n'}Z(k',i\omega_{n'})]^2-[\varepsilon_{k'}+\chi(k',i\omega_{n'})]^2}, \quad (2.20)$$

where the interaction kernel $I_l(k,i\omega_n;k',i\omega_{n'})$ is defined as

$$I_s(k,i\omega_n;k',i\omega_{n'})=\tfrac{1}{2}\int_0^{\pi}\sin\gamma\, d\gamma[V(|\mathbf{k}-\mathbf{k}'|)+V_+(|\mathbf{k}-\mathbf{k}'|)^2Q_+(|\mathbf{k}-\mathbf{k}'|,i\omega_n-i\omega_{n'})$$
$$-3V_-(|\mathbf{k}-\mathbf{k}'|)^2Q_-(|\mathbf{k}-\mathbf{k}'|,i\omega_n-i\omega_{n'})], \quad (2.21)$$

for s-wave pairing and

$$I_p(k,i\omega_n;k',i\omega_{n'})=\tfrac{1}{2}\int_0^{\pi}\sin\gamma\, d\gamma\cos\gamma[V(|\mathbf{k}-\mathbf{k}'|)+V_+(|\mathbf{k}-\mathbf{k}'|)^2Q_+(|\mathbf{k}-\mathbf{k}'|,i\omega_n-i\omega_{n'})$$
$$+V_-(|\mathbf{k}-\mathbf{k}'|)^2Q_-(|\mathbf{k}-\mathbf{k}'|,i\omega_n-i\omega_{n'})], \quad (2.22)$$

for p-wave pairing. Here γ is the angle between $\mathbf{k}$ and $\mathbf{k}'$. Note that although various states[27,28] may exist for p-wave pairing, the equation to determine T_c is the same for all those states.

F. Numerical procedure

Fortunately, the gap equation (2.20) has just the same structure as the corresponding one in the RPA. Thus we can apply the numerical techniques in Ref. 13 to the present case. The basic strategy of the techniques is to divide the k integral from 0 to ∞ into the sum of small appropriate intervals (k_i,k_{i+1}). A similar division is done for the ω_n sum. Then the integral equation is transformed into a matrix one with the inclusion of proper asymptotic behaviors. A power method is used to obtain the eigenvalues and eigenfunctions of the large-dimensional matrix. Those eigenvalues are used to determine T_c.

As for the self-energy part, no self-consistent treatment was done in Ref. 13, but (2.17) requires it. At each iteration step, however, we can use essentially the same techniques to calculate (2.17) as those in Ref. 13: Care is taken to treat the sharp peak in the Green's function $G(k,i\omega_n)$ at $k=k_F$ and $\omega_n\to 0$ as well as the long-range nature of the Coulomb interaction $V(q)$ at $q\to 0$. As usual, a division is made to the contribution of the level shift $\chi(k,i\omega_n)$ into the Fock part $\chi^F(k)$ and the correlation part $\chi^c(k,i\omega_n)$. The former is defined with the use of the bare interaction $V(|\mathbf{k}-\mathbf{k}'|)$ and the bare Green's function $G^{(0)}(k',i\omega_{n'})$ in (2.17), while the latter is the difference between $\chi(k,i\omega_n)$ and $\chi^F(k)$. The Fock part is independent of $i\omega_n$ and is given analytically as

$$\chi^F(k)=-\frac{2}{\pi}\alpha r_s\left[1+\frac{k_F^2-k^2}{2k_Fk}\ln\frac{k+k_F}{|k-k_F|}\right], \quad (2.23)$$

in units of E_F at $T=0$. Since the T dependence of the self-energy is weak for small enough T, say, $T\lesssim 0.05E_F$, we calculate $\chi^c(k,i\omega_n)$ and $Z(k,i\omega_n)$ only at $T=0.01E_F$ and an interpolation is used to obtain the values at different T with different values of ω_n. About 10 to 20 iteration steps are necessary to get the self-consistent self-energy. We consider the result converged if the relative error becomes less than 10^{-4} at each (k,ω_n) point.

In evaluating $\chi^c(k,i\omega_n)$ and $Z(k,i\omega_n)$ at $T\neq 0$, we have used the values at zero temperature for $\Pi(q,i\omega_m)$ in (2.6) in order to make the time for integration short. At $T=0$, $\Pi(q,i\omega_m)$ is calculated analytically as

$$\Pi(q,i\omega_m)=\frac{m^*k_F}{2\pi^2}P\left[\frac{q}{2k_F},\frac{m^*\omega_m}{qk_F}\right], \quad (2.24)$$

with $P(z,u)$, given by

$$P(z,u)=1+\frac{1-z^2+u^2}{4z}\ln\frac{(1+z)^2+u^2}{(1-z)^2+u^2}-u\tan^{-1}\frac{2u}{u^2+z^2-1}. \quad (2.25)$$

The branch of $\tan^{-1}z$ is chosen in the range $0-\pi$. This simplification does not cause any problem, because we are concerned with the case of T much lower than E_F. At most, we treat the situation with $T\approx 0.04E_F$, as we shall see in Sec. IV.

III. NORMAL-STATE PROPERTIES

Qualitative features of $\chi(k,i\omega_n)$ and $Z(k,i\omega_n)$ are the same as those in Fig. 1 of Ref. 13, whether they are calculated self-consistently or not. Thus we do not show the figures for them in the whole (k,ω_n) space here. Quantitatively, however, the values of those quantities are much different from those in Ref. 13, especially near the Fermi surface, i.e., at $k\approx k_F$ and $\omega_n\approx 0$. As an example to show the difference, we consider the chemical-potential shift due to the correlation $\mu_c\equiv\chi^c(k_F,0)$. In Fig. 1, μ_c in units of E_F is plotted as a function of r_s. The solid and dotted-dashed curves give, respectively, the results in the KO-G and KO-$G^{(0)}$ schemes. (Those schemes are explained in Sec. II D.) The dashed curve shows the results in the RPA given in Ref. 13, while the dotted one represents those of the Green's function Monte Carlo (GFMC) method.[29] Note that the GFMC gives virtually exact values for μ_c derived from the derivative of the correlation energy with respect to r_s.[20] The KO-$G^{(0)}$ scheme is found to reproduce almost exact μ_c in a very wide range of r_s. The RPA accounts for too large correlation effect, whereas the self-consistent KO-G procedure reduces the effect too much for this quantity. If we compare them with the results in BR, which are given in Fig. 4 of Ref. 12, we see that our results for μ_c in the KO-G scheme agree well with those indicated by KO1. (BR gives two kinds of results indicated by KO1 and KO2, but the physically acceptable model corresponds only to KO1. The model of KO2 is only an *ad hoc* one to obtain just better values of μ_c.)

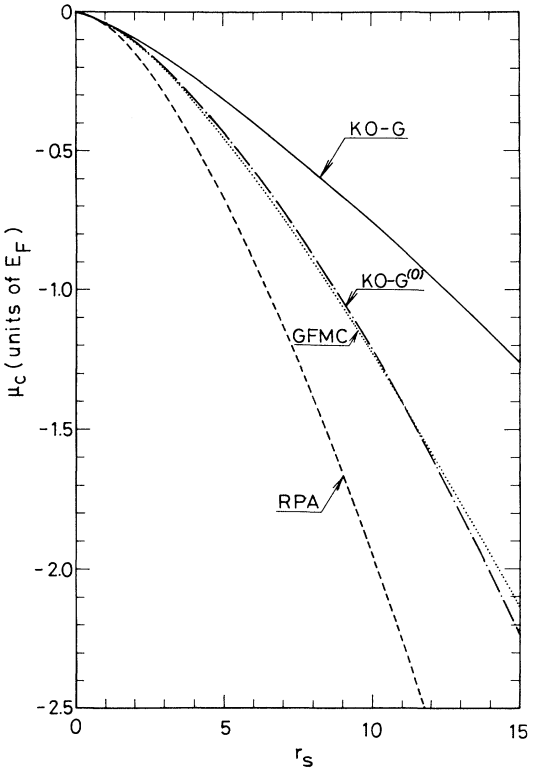

FIG. 1. Chemical-potential shift due to correlation μ_c in units of E_F as a function of r_s. The curves indicated by KO-G, KO-$G^{(0)}$, RPA, and GFMC represent, respectively, the results with the self-energy in (2.17), with the bare Green's function in (2.17), in the RPA, and in the GFMC (Refs. 20 and 29). The last method is considered to give virtually exact results.

A detailed comparison is also made for the quantities such as the renormalization factor at the Fermi level $z_F\equiv Z(k_F,0)^{-1}$ and the quasiparticle mass $\tilde{m}^*$, defined by

$$\frac{\tilde{m}^*}{m^*}\equiv\lim_{\omega_n\to 0}Z(k_F,i\omega_n)\Big/\left[1+\frac{\partial\chi(k_F,i\omega_n)}{2k_F\partial k_F}\right]. \quad (3.1)$$

As for z_F in the electron gas, the effective-potential expansion (EPX) method is known to provide the results very close to the exact values at least at metallic densities (i.e., $0<r_s<6$).[26] Compared to the EPX results, we find that the KO-$G^{(0)}$ scheme gives much better values for z_F than the KO-G scheme. In the latter scheme, the values for z_F are too large. Due primarily to this largeness of z_F, the values of $\tilde{m}^*$ in this scheme become definitely too small, but they agree well with those indicated by KO1 of BR in Fig. 3 of Ref. 12.

We note two points concerning the good agreement of the values for μ_c and $\tilde{m}^*$ between the self-consistent KO-G calculation and the one by BR: First, the agreement is obtained even though BR employed a different

form of $G_{\pm}(q)$ from ours. This indicates that the very details of $G_{\pm}(q)$ do not have serious effects on physical quantities. This has already been noted by BR, who tested various forms of the local-field correction including the ω-dependent one.[30] Second, BR neglected the contribution of transverse spin fluctuations, but no appreciable difference is found. This suggests that the contribution of those spin fluctuations is indeed small in the electron gas.

The self-consistent KO-G scheme is found to give worse values for the quantities at the Fermi surface than KO-$G^{(0)}$. We mention this possibility in Sec. II D by referring to the cancellation due to DuBois.[25] However, KO-$G^{(0)}$ is not necessarily a better procedure to calculate T_c: Consider the polaron problem. The energy at the Fermi level, which corresponds to the polaron ground-state energy, can be obtained more accurately by the use of $G^{(0)}$ [which amounts to the Rayleigh-Schrödinger (RS) perturbation theory] than the self-consistent G [which is equivalent to the Brillouin-Wigner (BW) scheme]. Nevertheless, a correct dispersion relation near the optic phonon energy can be given only when G is employed.[31] We can expect a similar situation for the processes at energies around ω_p that is much larger than E_F in the dilute electron gas. Probably KO-G, or the BW theory, is more appropriate to describe the quantities relating to the energy range larger than E_F, because the single-particle states with $\varepsilon_k < E_F$ may be regarded as degenerate in this energy range. For perturbation with degenerate states, we have to use BW rather than RS. Thus, if T_c in the plasmon mechanism is determined mainly by high-energy processes, KO-G is superior to KO-$G^{(0)}$.

IV. SUPERCONDUCTING PROPERTIES

Before we show the results of T_c, we point out the presence of the region in (q,ω) plane, where the real part of $V_{\sigma,\sigma'}(q,\omega)$ in (2.5) is *negative*. In Fig. 2, the hatched areas enclosed by the solid curves show those regions for singlet pair. [The case of $r_s=5$ is given in (a) and an extreme case of $r_s=40$ in (b).] The regions are associated with the plasmons, or the effect of charge fluctuations in (2.5). The same effect produces the regions of $\mathrm{Re}[V_{\sigma,\sigma'}(q,\omega)]<0$ for triplet pairing, which are enclosed by the dotted curves in Fig. 2. Those two regions are almost the same. In fact, for $r_s=5$, we cannot see the difference between the solid and dotted curves on the scale of the figure. Equation (2.22) shows clearly that spin fluctuations provide an additional attractive potential for triplet pair, though they give a repulsive one for single pair as shown in (2.21). This spin-fluctuation effect, however, cannot be a dominant process to cause superconductivity, because it does not produce a region

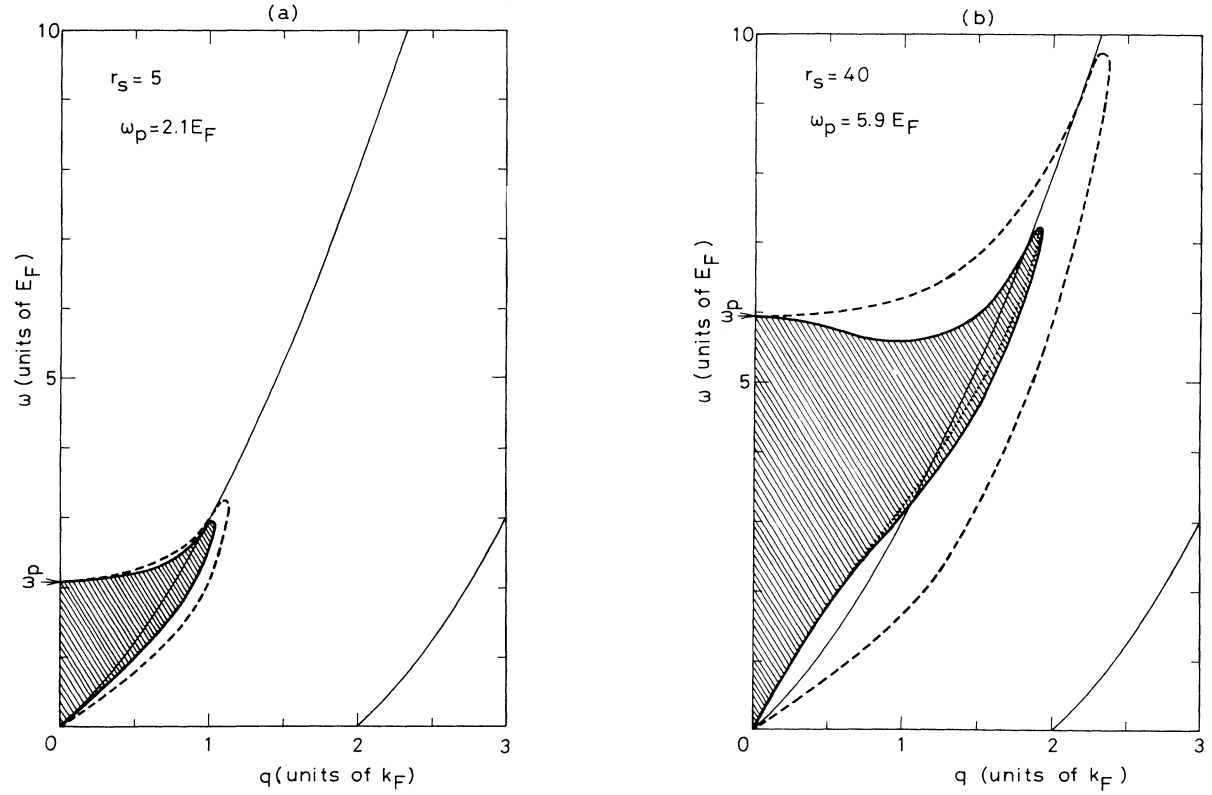

FIG. 2. Regions where the real part of the effective electron-electron interaction (2.5) is *negative* in (q,ω) plane for (a) $r_s=5$ and (b) $r_s=40$. The values of ω_p/E_F are, respectively, 2.1 and 5.9 for (a) and (b). The hatched areas enclosed by the solid and dotted curves indicate, respectively, the region of $\mathrm{Re}[V_{\sigma,\sigma'}(q,\omega)]<0$ for singlet and triplet pairs, while the areas surrounded by the dashed curves show the regions in the RPA. In each case, the thin solid curves give the boundaries for the single-particle excitations.

in which the whole effective interaction $V_{\sigma,\sigma'}(q,\omega)$ becomes negative. All it can do is to make the positive static interaction smaller for triplet pair than that for singlet pair. In any case, though it gives a little smaller area than that in the RPA shown by the dashed curve, the KO model still provides an attractive interaction over a very wide region in (q,ω) plane due to the plasmons. The region becomes wider as r_s increases. Thus we can expect the appearance of the plasmon mechanism of superconductivity in the large-r_s case.

This expectation is confirmed by the faithful solution of (2.20). Whether we employ the KO-G scheme or KO-$G^{(0)}$, we can always find superconducting solutions with $T_c/E_F > 10^{-4}$ for both s- and p-wave pairings, if we take r_s larger than 9. From the obtained values of T_c, we can determine the negative values of μ_F^* through the definition of

$$T_c \equiv 1.134 E_F \exp(1/\mu_F^*). \tag{4.1}$$

By extrapolating the data for μ_F^* to find the point of $\mu_F^*=0$, we can determine the critical value of r_s, r_{sc}, at which superconductivity begins to occur. The value of r_{sc} depends on the pairing nature as well as the scheme for $\Sigma(k,i\omega_n)$: For s-wave pairing, $r_{sc}=5.3$ for KO-G, while it is 4.8 for KO-$G^{(0)}$. We have similar r_{sc} values for p-wave pairing: $r_{sc}=3.3$ and 3.8 for KO-G and KO-$G^{(0)}$, respectively. Thus, if we increase r_s from zero, we find p-wave pairing first. However, at such a large value as $r_s=10$, s-wave pairing has higher T_c. This indicates the transition from p- to s-wave pairing at some critical r_s, which will be denoted by r_{st}. We determine r_{st} by the point at which μ_F^* for s-wave becomes equal to that for p-wave. Like r_{sc}, r_{st} depends on the calculation scheme. It is 4.7 for the RPA,[13] 8.6 for KO-G, and 8.2 for KO-$G^{(0)}$. The situation is summarized in Fig. 3 in which the

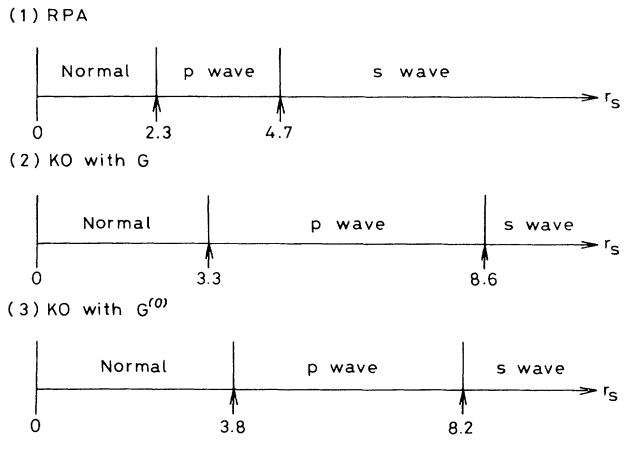

FIG. 3. Change of the phases with the increase of r_s in the ground state of the electron gas. The words "Normal", "p-wave", and "s-wave" correspond, respectively, to the normal state, the p-wave superconducting state, and the s-wave superconducting state. Case (1) shows the results in the RPA. Cases (2) and (3) show the present results with $\Sigma(k,i\omega_n)$ determined self-consistently for the former and with $\Sigma(k,i\omega_n)$ evaluated with the bare Green's function for the latter.

change of the ground state in the electron gas with the increase of r_s is shown.

Basically, the plasmons exist only in the small-q region for $\omega_p/E_F \leq 2$, i.e., $r_s \lesssim 5$ as seen in Fig. 2(a). In such a case, p-wave pairing can avoid the repulsive interaction for large-q processes more effectively than s-wave pairing, although the attractive interaction works almost equally to both of these pairings. For this reason, we have p-wave pairing in the small-r_s region even in the RPA as discussed in Ref. 13. In the present KO model, r_{sc} becomes larger, because the region of the attractive interaction decreases as shown in Fig. 2. The region for p-wave pairing, $r_{st}-r_{sc}$, is widened due primarily to the fact that the KO model suppresses s-wave pairing more strongly than p-wave pairing because of the repulsive spin-fluctuation term in (2.21). The p- to s-wave phase transition has already been predicted by Küchenhoff and Wölfle,[9] but the values for r_{sc} and r_{st} are very different. In their estimate, $r_{sc}=10$ and $r_{st}=35$. The prediction of such very large values of r_{sc} and r_{st} stems from the fact that they did not take a proper account of the dynamical effect, or the plasmon effect, on superconductivity.

The overall behavior of obtained $\phi_l(k,i\omega_n)$ is the same as given in Figs. 4 and 5 in Ref. 13. The most important feature is that ϕ_s extends over the very wide range in (k,ω_n) space, while ϕ_p tends to localize near the Fermi surface. This indicates that all the electrons inside the Fermi sphere participate in s-wave pairing, whereas only the electrons near the Fermi surface is involved in the formation of p-wave pairing. Combining the behavior of ϕ_s in (k,ω_n) space with the discussion on the different scheme for $\Sigma(k,\omega_n)$ in Sec. III, we consider that the KO-G scheme is definitely a better treatment for s-wave pairing, which needs a correct dispersion relation in a wide energy range. Such a clear view cannot be drawn for p-wave pairing, but KO-$G^{(0)}$ is probably preferable, because it produces a better dispersion relation near the Fermi surface. Thus, we consider that $r_{sc}=3.8$ is closer to reality than 3.3 for p-wave superconductivity. As for r_{st}, we have to compare the value of μ_F^* for s-wave pairing in KO-G with that for p-wave in KO-$G^{(0)}$ and find that $r_{st}\approx 8.5$.

In Figs. 4(a) and (b), we plot T_c as a function of r_s for s- and p-wave pairings, respectively, in the RPA (the dashed curves), the KO-G scheme (the solid curves), and the KO-$G^{(0)}$ scheme (the dotted-dashed curves) in units of effective kelvin K*. The features of all the curves are the same: As r_s increases, T_c increases rapidly first, reaches its maximum, and then decreases slowly. The latter decrease of T_c is associated with the decrease of the energy scale E_F. The strength of superconducting instability itself always increases with the increase of r_s. This can be seen either by the curve for T_c/E_F or equivalently μ_F^*. In Fig. 5, we show the values of μ_F^* for s-wave pairing as a function of r_s in various approximations. In any approximation, μ_F^* decreases monotonically. For large r_s, μ_F^* tends to be saturated, which indicates the linear relation between T_c and E_F. In fact, for $r_s \gtrsim 40$, or $E_F \lesssim 400$ K*, T_c for s-wave pairing in KO-G, the recommended one, is given approximately by $0.04E_F$. The maximum attain-

able temperature is found to be about 15 K* at $r_s \approx 25$. On the other hand, though it is predicted to occur in the region of $3.8 < r_s < 8.5$, p-wave pairing has only a very low T_c, i.e., of the order of 0.1 K* at the most.

We admit that the values of r_{sc} and r_{st} and consequently those of T_c in the region of r_s less than, say, 10 are not so reliable, because they depend on the approximation scheme. However, for $r_s > 40$ in which $\omega_p / E_F > 6$, T_c in KO-G is very close to that in the RPA as can be seen in Fig. 4(a), even though a lot of vertex corrections are included in the KO-G scheme through the local-field correction $G_{\pm}(q)$. Actually, we have already found a similar fact in Ref. 13: The variational calculation in the EPX method[7] has included more than 50 vertex corrections systematically, but the resulting T_c is virtually the same as that in the RPA for $r_s > 15$. This can be seen in Fig. 5 by comparing the dotted curve for μ_F^* with the dashed one. Thus all those calculations give the same values of T_c at least for $r_s > 40$. This suggests that the calculated T_c in this region is reliable.

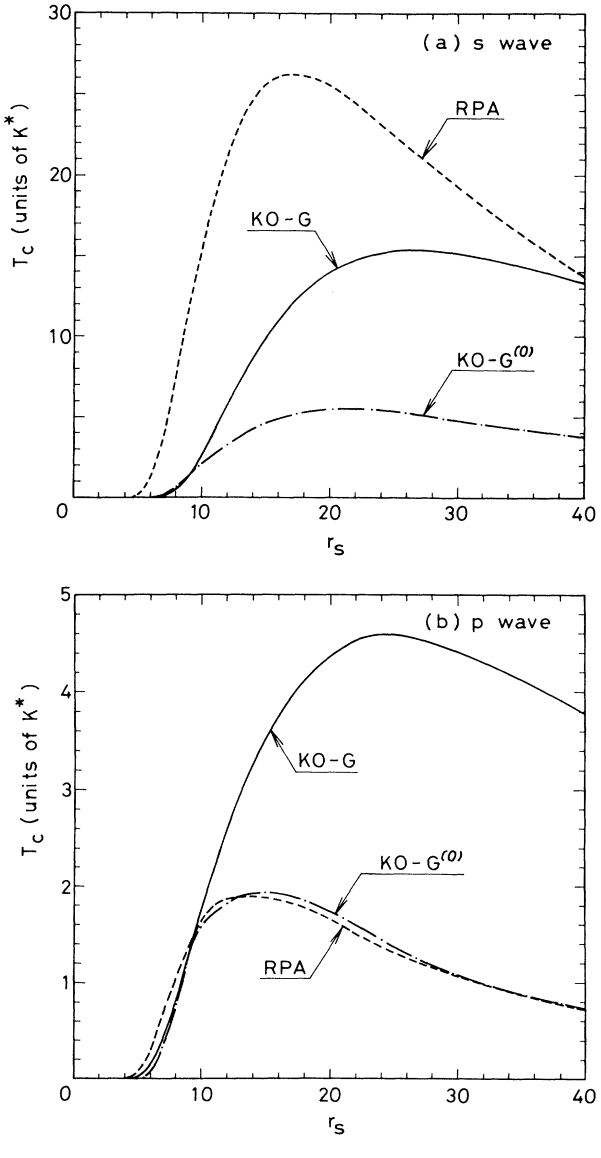

FIG. 4. Calculated results for T_c as a function of r_s for (a) s- and (b) p-wave pairings in the RPA (the dashed curves), the KO-G scheme (the solid curves), and the KO-$G^{(0)}$ scheme (the dotted-dashed curves) in units of effective kelvin K*. Note the difference in scales for T_c in (a) and (b).

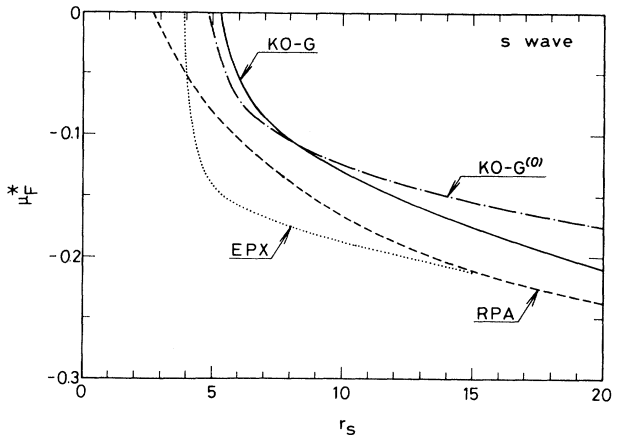

FIG. 5. Results of $\mu_F^* \equiv 1/\ln(T_c/1.134E_F)$ as a function of r_s for s-wave pairing in the RPA (the dashed curve, Ref. 13), the KO-G scheme (the solid curve), the KO-$G^{(0)}$ scheme (the dotted-dashed curve), and the EPX (the dotted curve, Ref. 7).

V. PHYSICAL CONSIDERATION OF THE PLASMON MECHANISM

Some two decades ago, Cohen discussed ineffectiveness of the plasmons on superconductivity.[32] He argued that the interaction kernel in the gap equation (2.2) took only care of the single-particle excitation region which hardly included the plasmons. (See Fig. 2.) Incorrectness of his argument can be seen by a mere consideration on the asymptotic behavior,[33] but here we review this problem from a different point of view, i.e., *the Coulomb hole,* in order to clarify a physical picture of the plasmon mechanism of superconductivity. Cohen's argument follows if we consider the contribution only from the poles of $G(k', \pm i\omega_{n'})$ in (2.2). In reality, however, the contribution from the poles of $\tilde{I}_{\sigma\sigma'}(\mathbf{k}, i\omega_n; \mathbf{k}', i\omega_{n'})$ should also be included even if those poles are off the pole region of $G(k', \pm i\omega_{n'})$. The plasmon pole involved in $\tilde{I}_{\sigma\sigma'}(\mathbf{k}, i\omega_n; \mathbf{k}', i\omega_{n'})$ is the principal effect that was overlooked by Cohen. The importance of this contribution has been realized in the normal-state properties as well:[34] In (2.17) to determine the self-energy, we have two important contributions. One is the screened-exchange term, which is the contribution from the pole of $G(k', i\omega_{n'})$ and the other is the Coulomb-hole term originating from the plasmon pole. Thus the faithful solution of (2.2) amounts to the evaluation of the Coulomb-hole effect on superconductivity.

The results in Sec. IV show clearly that this Coulomb-hole effect is strong enough to bring about superconductivity in the dilute electron gas. The coherent length of the present pair is short due to the rather large value of

T_c/E_F, which is around 0.04 for $r_s \approx 40$. This result can be extrapolated straightforwardly into a more dilute region. In a very dilute electron gas, on the other hand, the ferromagnetic and Wigner-crystal phases are predicted to occur. For example, an estimate exists that the former phase appears at $r_s = 75$, while the latter at $r_s = 100$.[29] In the ferromagnetic case, we will have no problem in the creation of p-wave pairing, but in the Wigner-crystal case, we cannot create either s- or p-wave pairing. However, we have obtained a rather clear view of the pairing mechanism in the dilute electron gas in the course of consideration on the relation between superconductivity and the Wigner crystal.

Let us consider the Wigner crystal in which each electron is confined to the lattice site by the potential $V(\mathbf{r})$ determined self-consistently. An approximate expression for $V(\mathbf{r})$ is given by[35]

$$V(\mathbf{r}) = -\frac{3}{2}\frac{e^2}{a_B^* r_s} + \frac{1}{2}\frac{e^2}{(a_B^* r_s)^3}\mathbf{r}^2. \tag{5.1}$$

This indicates that the electron makes a harmonic oscillation with the frequency $\omega \equiv [e^2/m^*(a_B^* r_s)^3]^{1/2} = \omega_p/\sqrt{3}$. As the electron density increases, other electrons penetrate into the region of the lattice site of the electron under consideration. This makes the restoring force for the oscillation weak and thus ω decreases. By the time ω is about the same as E_F, the Wigner crystal melts. But at that time, each electron oscillates with the frequency ω, which lies between E_F and ω_p. If we combine this fact with the attractive-interaction region in (q,ω) space in Fig. 2, we can expect that the effective interaction between electrons is mostly attractive. Thus, superconductivity may occur as soon as the Wigner crystal melts.

The fact that each electron in the Wigner crystal oscillates with a frequency as high as $\omega_p/\sqrt{3}$ is also useful in understanding the reason why the pair with a short coherent length is created in the dilute electron gas. (Even if the Wigner crystal is not created in the region of r_s around 40, the local environment due to the correlation effect is more or less the same for each electron.) We can regard the oscillation of an electron as the dissociation of the electron site from its accompanying Coulomb-hole site: At metallic densities, it is well known that the center of the Coulomb hole is always the same as the site of the original electron. In the Wigner crystal, however, the center of the Coulomb hole is the lattice site, or the origin $\mathbf{r}=\mathbf{0}$ in the potential $V(\mathbf{r})$, while the electron moves around it. Therefore, the site of the Coulomb hole is not determined by a temporal but the average position of the electron. (This situation is very similar to the polaron in the strong-coupling limit.) Thus, if temporarily, an electron goes into a rather distant place from the site of the Coulomb hole, the vacant site works as a very strong attractive center for another electron and pulls it. If the temporal absence of an electron occurs coherently with the attraction of another electron by the vacant Coulomb hole, this gives rise to the pair formation mediated by the Coulomb hole. We believe that this is the origin of superconductivity in the dilute electron gas.

VI. SUMMARY AND DISCUSSION

In this paper, we have discussed superconductivity in the dilute electron gas by solving the full Eliashberg equation in which the KO model is used to determine both the one-particle Green's function and irreducible electron-electron interaction with the exchange and correlation effects. The plasmon mechanism of superconductivity is found to exist. The p- to s-wave transition is predicted as r_s increases. For $r_s > 40$, we obtain the result of $T_c \approx 0.04 E_F$ for s-wave pairing. This value of T_c is rather insensitive to the approximations used in the calculation. The physical origin of this superconductivity is explained with the concept of the Coulomb hole, which has been rather useful in expressing the plasmon effect on the normal-state self-energy. The pairing mechanism mediated by this Coulomb hole is suggested and a possible direct transition from the superconducting phase to the Wigner-crystal one is mentioned.

In order to understand why the value of T_c/E_F is insensitive to the vertex corrections in the dilute electron gas, a Migdal's-type theorem is considered recently by an analytical calculation at the limit $\omega_p/E_F \gg 1$.[36] For r_s less than about 15 where the vertex corrections have important effects, we find a totally different situation between the EPX and KO-G: The vertex corrections included in KO-G suppress T_c as a whole, while those in the EPX enhance it. At present no one knows which is closer to reality, but this arises from the different treatment of the energy denominators in the vertex corrections. The ω-dependent vertex corrections are included rather faithfully in the EPX, while this is not the case for KO-G in the formalism with $G_{\pm}(q)$.

The value of $T_c \approx 0.04 E_F$ in the low-E_F region agrees quantitatively with the result of Uemura and coworkers,[37,38] who claim that all the exotic superconductors including the copper-oxides, heavy fermions, organic materials, and the alkali-metal-doped C_{60} can be characterized experimentally by the universal fact that T_c is roughly in proportion to E_F with the coefficient of about 0.04. As mentioned in Refs. 13 and 36, the plasmon mechanism, which can work, in principle, in all the charged systems is very favorable to explain such a universal relation, if any. In order to explain the variations of T_c from the universal relation in each class of the materials, we should add other mechanisms such as phonons, excitons, and magnetic fluctuations to the plasmon mechanism and this is an important future problem.

In the plasmon mechanism, superconductivity occurs more easily as ω_p/E_F becomes larger. It is of interest to note that an approach based on the renormalization group suggests that superconductivity cannot appear in the model with a purely repulsive bare interaction if the renormalization starts with the low-energy weak-coupling region.[39] We suggest that the renormalization-group technique should be employed with the inclusion of the high-energy plasmon effect to reconfirm the plasmon mechanism. We also suggest that the GFMC-type calculation might be done to find the superconducting solution in the low-density electron gas. The search

for a transition from the Wigner crystal to superconductivity would be very exciting.

In the electron-gas model, the insulating phase in the strong-correlation region is the Wigner crystal, while in the lattice models such as the Hubbard model, the corresponding one is the Mott-Hubbard insulating phase. Extension of the concept of the Coulomb-hole mediation to the lattice models might be interesting.

[1]W. Kohn and J. M. Luttinger, Phys. Rev. Lett. **15**, 524 (1965).
[2]Y. Takada, J. Phys. Soc. Jpn. **45**, 786 (1978).
[3]H. Rietschel and L. J. Sham, Phys. Rev. B **28**, 5100 (1983).
[4]M. Grabowski and L. J. Sham, Phys. Rev. B **29**, 6132 (1984).
[5]L. J. Sham, Physica B **135**, 451 (1985).
[6]J. J. Shirron and J. Ruvalds, Phys. Rev. B **34**, 7596 (1986).
[7]Y. Takada, Phys. Rev. B **37**, 155 (1988).
[8]M. Grabowski and L. J. Sham, Phys. Rev. B **37**, 3726 (1988).
[9]S. Küchenhoff and Wölfle, Phys. Rev. B **38**, 935 (1988).
[10]G. S. Canright and G. Vignale, Phys. Rev. B **39**, 2740 (1989).
[11]Y. Takada, Phys. Rev. B **39**, 11 575 (1989).
[12]T. Büche and H. Rietschel, Phys. Rev. B **41**, 8691 (1990).
[13]Y. Takada, J. Phys. Soc. Jpn. **61**, 238 (1992).
[14]G. H. Eliashberg, Zh. Eksp. Teor. Fiz. **38**, 966 (1960) [Sov. Phys. JETP **11**, 696 (1960)].
[15]J. P. Eisenstein, L. N. Pfeiffer, and K. W. West, Phys. Rev. Lett. **68**, 674 (1992).
[16]A. B. Migdal, Zh. Eksp. Teor. Fiz. **34**, 1438 (1958) [Sov. Phys. JETP **7**, 996 (1958)].
[17]C. A. Kukkonen and A. W. Overhauser, Phys. Rev. B **20**, 550 (1979).
[18]G. Niklasson, Phys. Rev. B **10**, 3052 (1974).
[19]X. Zhu and A. W. Overhauser, Phys. Rev. B **30**, 3158 (1984).
[20]S. H. Vosko, L. Wilk, and M. Nusair, Can. J. Phys. **58**, 1200 (1980).
[21]H. Yasuhara, Solid State Commun. **11**, 1481 (1972).
[22]Y. Takada, Phys. Rev. B **43**, 5979 (1991).
[23]G. Vignale and K. S. Singwi, Phys. Rev. B **32**, 2156 (1985).
[24]T. K. Ng and K. S. Singwi, Phys. Rev. B **34**, 7738 (1986); **34**, 7743 (1986).
[25]D. F. DuBois, Ann. Phys. (N.Y.) **7**, 174 (1957); **8**, 24 (1959). See also, a recent paper, H. Yasuhara and Y. Takada, Phys. Rev. B **43**, 7200 (1991).
[26]Y. Takada and H. Yasuhara, Phys. Rev. B **44**, 7879 (1991).
[27]P. W. Anderson and P. Morel, Phys. Rev. **123**, 1911 (1961).
[28]R. Balian and N. R. Werthamer, Phys. Rev. **131**, 1553 (1963).
[29]D. M. Ceperley and B. J. Alder, Phys. Rev. Lett. **45**, 566 (1980).
[30]B. Dabrowski, Phys. Rev. B **34**, 4989 (1986).
[31]G. Whitfield and R. Puff, Phys. Rev. **139**, A338 (1965).
[32]M. L. Cohen, in *Superconductivity*, edited by R. D. Parks (Marcel Dekker, New York, 1969), Vol. 1, Chap. 12, p. 659.
[33]Y. Takada, J. Phys. Soc. Jpn. **49**, 1267 (1980).
[34]L. Hedin, Phys. Rev. **139**, A796 (1965).
[35]D. Pines, in *Elementary Excitations in Solids* (Benjamin, New York, 1964), Chap. 3-3.
[36]Y. Takada, J. Phys. Soc. Jpn. **61**, 3849 (1992).
[37]Y. J. Uemura, L. P. Le, G. M. Luke, B. J. Sternlieb, W. D. Wu, J. H. Brewer, T. M. Riseman, C. L. Seaman, M. B. Maple, M. Ishikawa, D. G. Hinks, J. D. Jorgensen, G. Saito, and H. Yamochi, Phys. Rev. Lett. **66**, 2665 (1991).
[38]Y. J. Uemura, A. Keren, L. P. Le, G. M. Luke, B. J. Sternlieb, W. D. Wu, J. H. Brewer, R. L. Whetten, S. M. Huang, S. Lin, R. B. Kaner, F. Diederich, S. Donovan, G. Grüner, and K. Holczer, Nature (London) **352**, 605 (1991).
[39]R. Shankar, Physica A **177**, 530 (1991).